Asian Journal of Chemistry; Vol. 26, No. 13 (2014), 3927-3931

ASIAN JOURNAL OF CHEMISTRY

http://dx.doi.org/10.14233/ajchem.2014.16037A

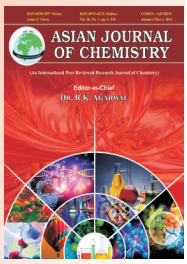

Synthesis of Mesoporous LTA Zeolite with Bridged Silsesquioxane as Template

HONG-TAO LIU, GUO-QIANG SONG, YING MENG and FU-XIANG LI*

Research Institute of Special Chemicals, Taiyuan University of Technology, Taiyuan 030024, Shanxi Province, P.R. China

*Corresponding author: Fax: +86 351 6111178; Tel: +86 351 6010550; E-mail: L63f64x@163.com

Received: 11 July 2013; *Accepted*: 12 September 2013; *Published online*: 23 June 2014; AJC-15376

In this paper, a mesoporous LTA zeolite with uniform intracrystal mesopores has been synthesized using the bridged silsesquioxane with three hydrolyzable methoxy silicon groups as the template, which can form Si-O-Si covalent bonds with the zeolite structure in undergoing nucleation. The structural and textural properties were characterized by X-ray diffraction, nitrogen adsorption, scanning electron microscopy and transmission electron microscopy. The XRD patterns of the as-synthesized samples clearly indicated a gradual decrease in the size of the crystalline domains as the amount of the template increases. The samples all showed a type IV N_2 adsorption-desorption isotherm characteristic of mesoporous materials and the pore size distribution centered at around 3.401-3.799 nm, confirming the presence of uniform intracrystal mesopores in the zeolite samples. SEM and transmission electron microscopy observations of the samples showed that the uniform and partially interconnected intracrystal mesopores randomly distributed throughout the globular particles with rugged surfaces.

Keywords: Bridged silsesquioxane, Mesoporous, Template, Synthesis, LTA zeolites.

INTRODUCTION

Zeolite molecular sieve is a kind of typical microporous solid materials with the crystalline structure. For its good ion exchange performance, strong acidity and extraordinary hydrothermal stability, zeolite molecular sieve is widely used in catalytic, adsorption and separation fields[1]. The excellent shape-selectivity of zeolite molecular sieve makes it used in particular reactions. However, the diffusion limitation of large molecule reactants into the micropore and large molecule products escaping from the holes, which results in that many catalytic processes are difficult to happen, greatly influences the spread of the actual application ranges[2,3].

The successful combination of the structured mesoporous materials effectively solved the problem of diffusion limitation in microporous zeolites. The catalytic active center can be fixed on the wall of mesopores by surface modification, so as to disperse the catalyst and heterogenize the homogeneous catalyst[4-12]. However, compared with conventional zeolites, the shortcomings of weak acidity and bad hydrothermal stability also limit the development of mesoporous materials with amorphous structure.

In recent years, many experts have been committed to coming up with the methods of synthesizing mesoporous zeolites. Such mesoporous zeolites contain, in addition to the crystallographic micropore system characteristic of zeolites, also an independent mesopore system and possessing not only strong acidity and extraordinary hydrothermal stability, but also the diffusion advantages of mesoporous materials. Owing to the improvement of mass-transport rate and catalytic performance, it is generally accepted that this kind of mesoporous zeolites will have a potentially industrial application prospect[13-30].

The research works of synthesizing mesoporous zeolites by carbon materials templating approach have been extensively carried out. Under different crystallization conditions, well crystallization mesoporous zeolites have been successfully synthesized with the above method. In general, the carbon materials templating approach can be templated in zeolite materials by using of carbon nanoparticles, carbon aerogels, porous carbons and so on[13-26]. As a conventional approach to introduce mesoporosity in zeolite materials, carbon materials templating approach is very important in providing diversity in structure of zeolites. However, by now, it is relatively difficult to synthesize intracrystalline mesopore system. Using the carbon materials templating approach prefers to form nano-sized zeolite aggregate with intergranular mesopore (diameter above 10 nm). Corresponding mesoporous aperture distribution is so wide that the adjustment of mesoporous structure is with limitations and the synthesised zeolites are lack of strong acidity and extraordinary hydrothermal stability. Some research institutions have reported that mesoporous zeolites were successfully synthesized by performing a direct hydrothermal synthesis using cationic polymers[27], amphiphilic organosilanes surfactants[28-29] or silicon alkylation polymers[30]. Compared with

conventional zeolite catalysts, the synthesised zeolites possess a tailored pore structure and remarkable products selectivity and catalytic activity, which have potential application value in aspects of macromolecular adsorption and catalysis.

In this paper, $(CH_3O)_3Si(CH_2)_3N[CH_2CHOHCH_2O(CH_2)_3Si(CH_3O)_3]_2$(named bridged silsesquioxane) was synthesized. A mesoporous LTA zeolite with uniform intracrystal mesopores has been synthesized using the bridged silsesquioxane as mesopore-generating agent by performing a direct hydrothermal synthesis.

Fig. 1 illustrates the proposed synthesis mechanism for mesoporous LTA zeolite with uniform intracrystal mesopores using bridged silsesquioxane as mesoporogen. Besides alkylammonium groups, bridged silsesquioxane also have three silicon groups with three hydrolyzable methoxy respectively, which connect together by Si-C bond and have good chemical stability in synthesis condition of zeolites. After bridged silsesquioxane was added to the initial synthesis composition of LTA zeolites, the methoxy silicon groups experienced a process of hydrolysis and SiO_3^- groups was produced; and the formation of Si-O-Si covalent bonds made it possible to connect the bridged silsesquioxane with the framework of the zeolites. Through calcination, the bridged silsesquioxane was removed, forming mesoporous LTA zeolites with uniform intracrystal mesopores (Fig. 1).

EXPERIMENTAL

Sodium aluminate ($NaAlO_2$, A.R) was purchased from Tianjin Guangfu Fine Chemical Research Institute. Sodium metasilicate nonahydrate ($Na_2SiO_3{\cdot}9H_2O$, A.R) was from Tianjin Fengchuan Chemical Reagent Science And Technology Co., Ltd. γ-aminopropyl trimethoxysilane $[NH_2(CH_2)_3Si(OCH_3)_3$, KH-540, A.R] and 2,3-epoxy propoxy propyltrimethoxy- silicane ($CH_2OCHCH_2O(CH_2)_3Si(OCH_3)_3$, KH-560, A.R) were both from TRUSTCHEM SILANES LTD.

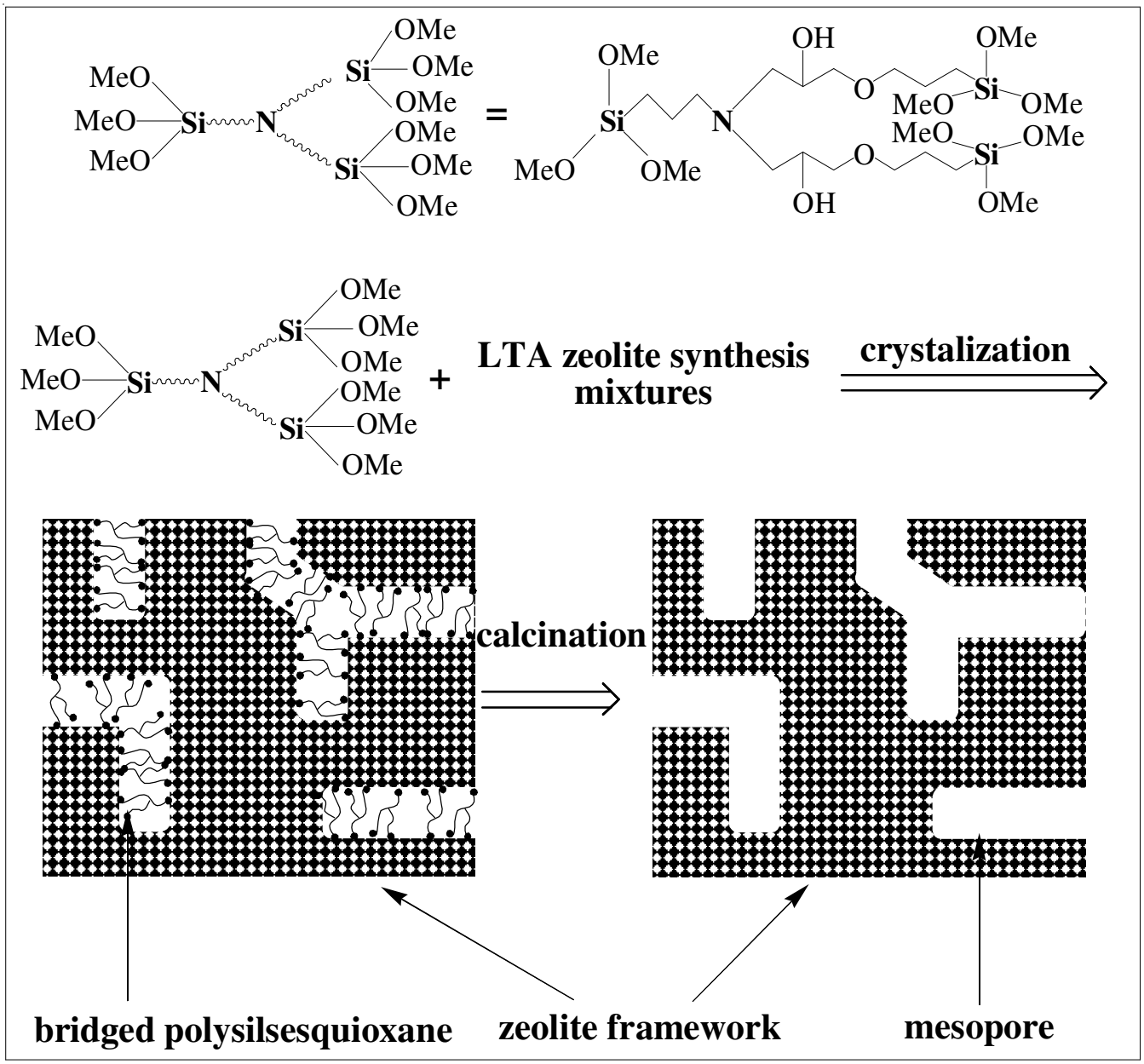

Fig. 1. Proposed synthesis mechanism for mesoporous LTA zeolite with uniform intracrystal mesopores using bridged silsesquioxane as mesoporogen

X-ray diffraction patterns were performed using an X-ray diffractometer (LabX XRD-6000, Shimadzu Corp) with a monochromatized Ni-filtered CuK_α radiation ($\lambda = 0.15418$ nm) X-ray beam and a generator voltage with current of 40 kV and 30 mA, respectively. The scanning angle is in the 2θ range of 5-35°.

The surface area and pore size distribution of the as-synthesized samples were determined by nitrogen adsorption-desorption measurements at 77 K (Quantachrome ASAP of Nova 2000e). The samples were outgassed in vacuum at 573 K for 3 h prior to measurements. The total surface area was calculated through the BET method. The pore size distribution and pore volume were analyzed based on the Barrett-Joyner-Halenda model.

Field emission scanning electron microscopys (SEM) (JSM-6700F and Hitachi S-4800) worked with the accelerating voltage of 10 kV and 5 kV, respectively, after the gold-plated processing in vacuum were conducted. Transmission electron microscopy (TEM) was performed on a Philips Tecnai G2 F20 at an accelerating voltage of 200 kV. Before measurement, the samples firstly dispersed in ethanol solution under ultrasonic and the mixture was added drop-wise on copper wire nets of the carbon load.

Preparation of the bridged silsesquioxane: The bridged silsesquioxane was synthesized using KH-560 and KH-540 as precursors(n(KH 540): n(KH 560) = 2:1). With the protection of N2, 22.5 mL KH 560 was added to a flask with a condenser, a dropping funnel and a thermometer. Then, after 8.5 mL KH 540 was added, the mixture was stirred vigorously for 48 h at 70 °C to obtain the straw yellow product, bridged silsesquioxane monomer (**Scheme-I**).

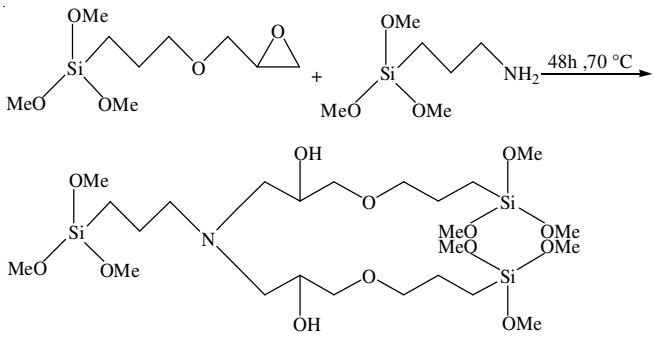

Scheme-I: Synthesis mechanism of bridged silsesquioxane (-Me: -CH_3)

Preparation of mesoporous LTA zeolite: In the procedure of mesoporous LTA zeolites, bridged silsesquioxane was added to a typical alkaline mixture of sodium silicate, sodium aluminate and distilled water. The molar composition of the mixture was 1.173 SiO_2·2.173 Na_2O·Al_2O_3·208 H_2O·nBS, where n varied in 0, 0.0813, 0.101, 0.126 and 0.151. The as-synthesized zeolite samples were denoted as LTA, mesoporous LTA-1, mesoporous LTA-2, mesoporous LTA-3 and mesoporous LTA-4.

In a typical synthesis of mesoporous LTA-4, 0.750 g sodium metasilicate nonahydrate was first dissolved in 4 mL distilled water. Then, 0.222 g bridged silsesquioxane was added drop-wise under vigorous stirring at 308 K and then a clear solution was obtained. Subsequently, the above solution was added drop-wise to a solution of 0.369 g $NaAlO_2$ dissoving in 4 mL distilled water. The final mixture was continuously stirred for 0.5 h at 308 K to obtain a homogeneous gel. The resultant gel was then crystallized hydrothermally for 192-288 h at 373 K in a Teflon-coated stainless-steel autoclave. The precipitated product was filtered by suction and then washed with distilled water until the pH of the filtrate to neutral. The product was dried in an oven at 373 K and then calcined in air for 10 h at 823 K to remove bridged silsesquioxane template.

RESULTS AND DISCUSSION

Fig. 2 shows the XRD patterns of the mesoporous LTA zeolites samples synthesized with different amounts of bridged silsesquioxane as mesoporogen. The patterns all exhibit the typical diffraction peaks of LTA zeolites, confirming that mesoporous LTA samples all have the same crystal structure as the conventional LTA zeolites. However, with bridged silsesquioxane quantity increase, the diffraction peak widths of mesoporous LTA samples gradually increase, while the peak intensities decrease. As the bridged silsesquioxane increase to a certain amount, the diffraction peaks almost disappear, indicating a gradual decrease in the size of the crystalline domain as the amount of the template increase.

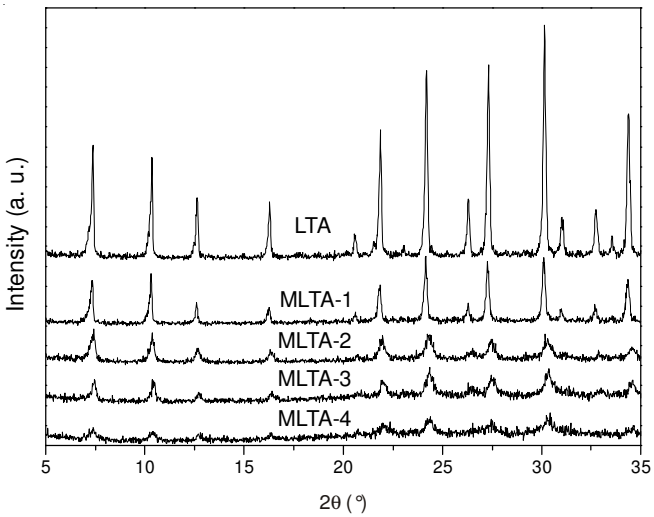

Fig. 2. Wide-angle XRD patterns of conventional LTA and mesoporous LTA samples

Fig. 3 shows the N_2 adsorption-desorption isotherms and corresponding pore size distribution curves of the as-synthesized mesoporous LTA samples. The isotherms all exhibit a type of IV isotherms characteristic of mesoporous materials. The adsorption branches have a steep increase in the range of $P/P_0 = 0.4$-0.9. A broad hysteresis loop appears in the range of $P/P_0 = 0.5$-0.98 and the hysteresis loop gradually increases with increased bridged silsesquioxane quantity, which is attributed to N_2 gas capillary condensation in the mesopores. The increased bridged silsesquioxane amounts are beneficial to generate more developed mesoporous structure. Correspondingly, the pore size analysis of all mesoporous LTA samples using barret-joyner-halenda algorithm shows a narrow pore size distribution centered at around 3.401-3.799 nm and increased bridged silsesquioxane amounts lead to more concentrated

pore size distribution, confirming the presence of uniform mesopores in mesoporous LTA samples. The pore textural properties of the as-synthesized mesoporous LTA samples are represented in Table-1. The mesopore volume as well as the BET surface area gradually increase as the amount of bridged silsesquioxane and reach to maximum of 0.109 $cm^3 g^{-1}$ and 61.254 $m^2 g^{-1}$, respectively. The above analysis supports the XRD conclusion and is a further indication that the mesoporous LTA samples have uniform intracrystal mesopores.

Fig. 4 shows the SEM images of the conventional LTA zeolites and mesoporous LTA samples. The conventional LTA zeolites possess perfect cubic crystal (Fig. 4a). With the addition of bridged silsesquioxane, the cubic crystal turns into a spherical crystal with rough surfaces and a particle size in 700 nm to 800 nm ranges, which can be observed from the low magnification SEM images (Fig. $4b_1$-c_1). In addition, the high resolution SEM images (Fig. $4b_2$-c_2) of the mesoporous LTA samples exhibit partial interconnected intracrystal mesopores existed in the zeolite particles. In conclusion, the addition of bridged silsesquioxane leads to a significantly decrease in crystal size and forms a distinctly different morphology with the conventional LTA zeolites.

The transmission electron microscopy images of mesoporous LTA-4 at high magnification (Fig. 5) further proof the existence of intracrystal mesopores in the mesoporous LTA zeolites. It can be observed clearly that larger light contrast areas randomly extends over the entire particle, indicating that the mesoporous LTA particles possess a highly developed mesoporous structure and the mesopores irregularly distribute in the whole zeolite particle. In addition, the mesoporous channels are partially interconnected, which has a good agreement with the results from the SEM observations. The

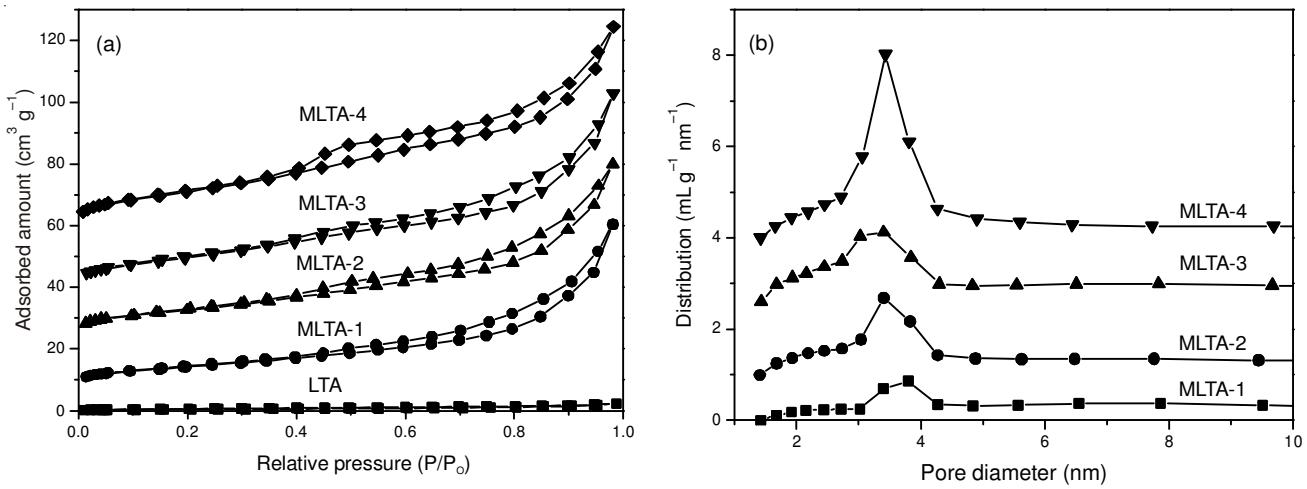

Fig. 3. (a) N_2 adsorption-desorption isotherms and (b) Barret-joyner-halenda pore size distributions curves of the mesoporous LTA samples. Included for comparison are the isotherm and corresponding pore size distribution of the conventional LTA zeolite synthesized with the same procedure but without bridged silsesquioxane

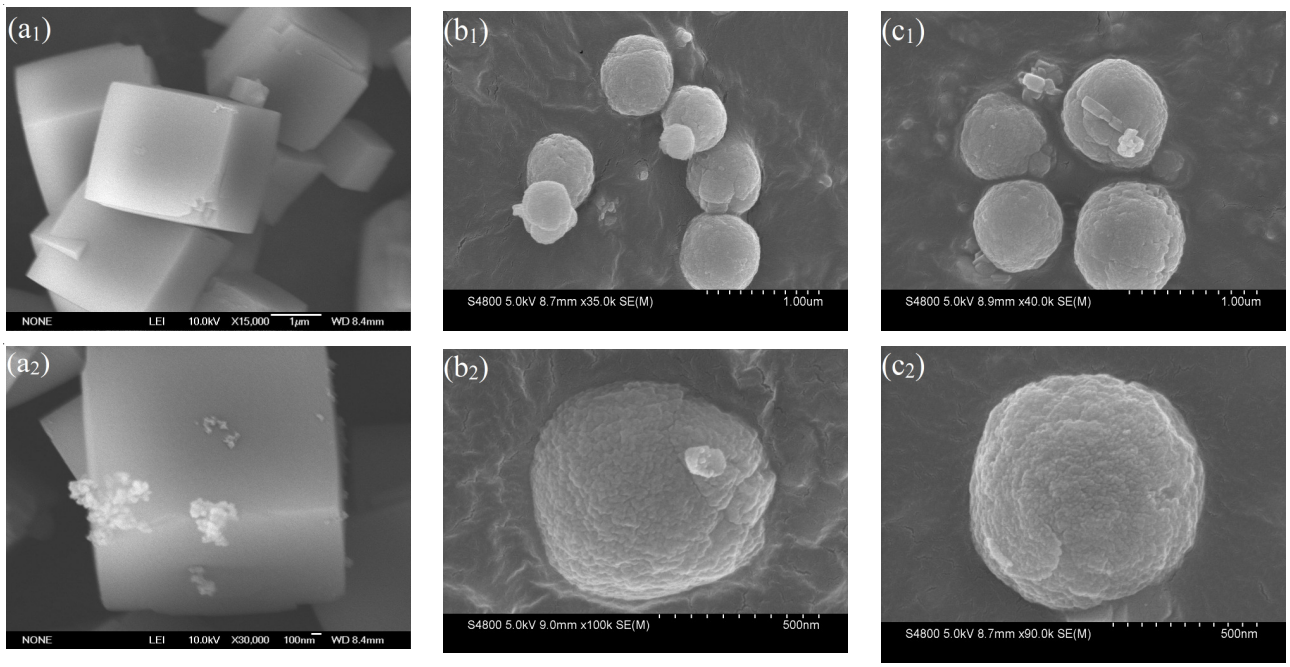

Fig. 4. SEM images of LTA and mesoporous LTA samples at low (left column) and high (right column) magnification, respectively. (a) LTA; (b) mesoporous LTA-3; (c) mesoporous LTA-4

TABLE-1
PORE TEXTURAL PROPERTIES OF THE MESOPOROUS LTA SAMPLES

Samples	S_{BET} ($m^2 g^{-1}$)*	V_{meso} ($cm^3 g^{-1}$)**	D_{BJH} (nm***)
Mesoporous LTA-1	32.976	0.085	2.3.799
Mesoporous LTA-2	42.028	0.092	3.403
Mesoporous LTA-3	52.813	0.104	3.401
Mesoporous LTA-4	61.254	0.109	3.434

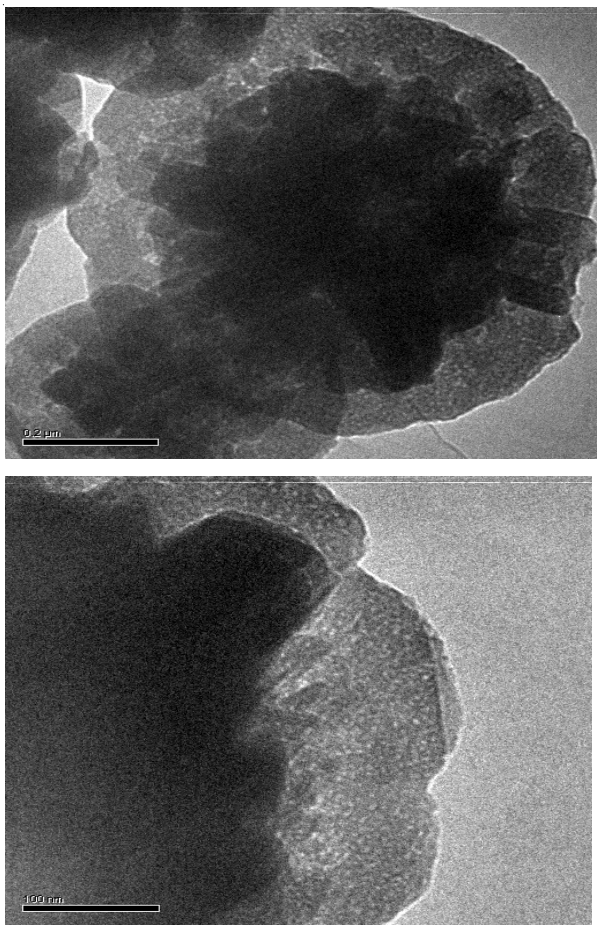

Fig. 5. Transmission electron microscopy images of mesoporous LTA-4 at high magnification. The light contrast areas indicate the presence of intracrystal mesopores

transmission electron microscopy images of mesoporous LTA-4 also show the nearly uniform size (about 2 nm) of intracrystal mesopores and the narrow pore size distribution is consistent with the detection from the N_2 adsorption-desorption isotherms.

Conclusion

In the present study, a mesoporous LTA zeolite, featuring of uniform intracrystal mesopores and concentrated pore size distribution, has been successfully synthesized using bridged silsesquioxane as the mesoporous structure-directing agent. The bridged silsesquioxane with the certain molecule structure used in this paper is not the only mesoporous structure-directing agent and other types of bridged silsesquioxane monomers also could be used to form developed intracrystal mesopores in zeolite. In addition, this approach could also be applied in the synthesis of other mesoporous zeolites with similar structure by choosing of suitable bridged silsesquioxane monomers. Owing to their superior structural performances, such as large BET surface area, large mesopore volume, uniform interconnected intracrystal mesopores and concentrated pore size distribution, these mesoporous zeolites will lead to numerous technical applications in catalysis, adsorption and separation.

ACKNOWLEDGEMENTS

This study was supported by the National Natural Science Foundation of China (50972097).

REFERENCES

1. A. Corma, *Chem. Rev*., **97**, 2373 (1997).
2. M.E. Davis, *Nature*, **417**, 813 (2002).
3. M. Hartmann, *Angew. Chem. Int. Ed*., **43**, 5880 (2004).
4. P.T. Tanev and T.J. Pinnavaia, *Science*, **271**, 1267 (1996).
5. Z. Zhang, Y. Han, F.S. Xiao, S. Qiu, L. Zhu, R. Wang, Y. Yu, Z. Zhang, B. Zou, Y. Wang, H. Sun, D. Yuan and Y. Wei, *J. Am. Chem. Soc.*, **123**, 5014 (2001).
6. D. Zhao, J. Feng and Q. Huo, N. Melosh, G.H. Fredrickson, B.F. Chmelka and G.D. Stucky, *Science*, **279**, 548 (1998).
7. S.P. Naik, T. Yokoi, W. Fan, Y. Sasaki, T.- Wei, H.W. Hillhouse and T. Okubo, *J. Phys. Chem. B*, **110**, 9751 (2006).
8. M. Ogura, H. Miyoshi, S.P. Naik and T. Okubo, *J. Am. Chem. Soc*., **126**, 10937 (2004).
9. C. Li, H.D. Zhang, D.M. Jiang and Q.H. Yang, *Chem. Commun.*, 547 (2007).
10. Y. Liu, W. Zhang and T.J. Pinnavaia, *J. Am. Chem. Soc.*, **122**, 8791 (2000).
11. Z. Zhang, Y. Han, L. Zhu, R. Wang, Y. Yu, S.L. Qiu, D.Y. Zhao and F.-S. Xiao *Angew. Chem. Int. Ed.*, **40**, 1258 (2001).
12. D.T. On and S. Kaliaguine, *Angew. Chem. Int. Ed*., **40**, 3248 (2001).
13. C.J.H. Jacobsen, C. Madsen, J. Houzvicka, I. Schmidt and A. Carlsson, *J. Am. Chem. Soc*., **122**, 7116 (2000).
14. G.L. Wood, E.A. Pruss and R.T. Paine, *Chem. Mater*., **13**, 12 (2001).
15. I. Schmidt, C. Madsen and C.J.H. Jacobsen, *Inorg. Chem*., **39**, 2279 (2000).
16. A.H. Janssen, I. Schmidt, C.J.H. Jacobsen, A.J. Koster and K.P. de Jong, *Micropor. Mesopor. Mater*., **65**, 59 (2003).
17. T.- Arima, *Nat. Mater*., **7**, 12 (2008).
18. K. Egeblad, M. Kustova, S.K. Klitgaard, K. Zhu and C.H. Christensen, *Micropor. Mesopor. Mater*., **101**, 214 (2007).
19. C. Chen, S. Wang, N. Zhang, Z. Yan and W. Pang, *Micropor. Mesopor. Mater*., **106**, 1 (2007).
20. M.A. Hortalá, L. Fabbrizzi, N. Marcotte, F. Stomeo and A. Taglietti, *J. Am. Chem. Soc*., **125**, 20 (2003).
21. Y. Tao, H. Kanoh, L. Abrams and K. Kaneko, *Chem. Rev*., **106**, 896 (2006).
22. Z. Yang, Y. Xia and R. Mokaya, *Adv. Mater*., **16**, 8 (2004).
23. Y. Fang and H. Hu, *J. Am. Chem. Soc*., **128**, 33 (2006).
24. Y. Fang and H. Hu, *Catal. Commun*., **8**, 817 (2007).
25. X. Wei and P.G. Smirniotis, *Micropor. Mesopor. Mater*., **89**, 170 (2006).
26. Y. Einaga, M. Taguchi, G. Li, T. Akitsu, Z. Gu, T. Sugai and O. Sato, *Chem. Mater*., **15**, 8 (2003).
27. F.S. Xiao, L. Wang, C. Yin, K. Lin, Y. Di, J. Li, R. Xu, D.S. Su, R. Schlögl, T. Yokoi and T. Tatsumi, *Angew. Chem. Int. Ed*., **45**, 3090 (2006).
28. M. Choi, H.S. Cho, R. Srivastava, C. Venkatesan, D.-H. Choi and R. Ryoo, *Nat. Mater*., **5**, 718 (2006).
29. R. Srivastava, M. Choi and R. Ryoo, *Chem. Commun.*, **43**, 4489 (2006).
30. H. Wang and T.J. Pinnavaia, *Angew. Chem. Int. Ed*., **45**, 7603 (2006).